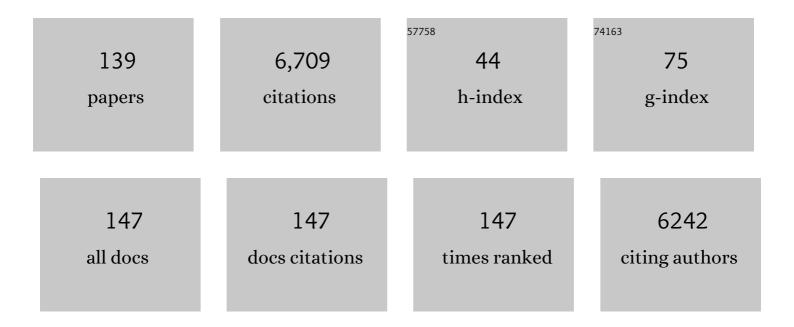
Markus Nilsson

List of Publications by Year in descending order

Source: https://exaly.com/author-pdf/3899423/publications.pdf Version: 2024-02-01



MADRILS NUSSON

#	Article	IF	CITATIONS
1	Histogram analysis of tensor-valued diffusion MRI in meningiomas: Relation to consistency, histological grade and type. NeuroImage: Clinical, 2022, 33, 102912.	2.7	11
2	Diffusion tensor imaging in glioblastoma patients treated with volumetric modulated arc radiotherapy: a longitudinal study. Acta Oncológica, 2022, 61, 680-687.	1.8	2
3	Post-Concussive Vestibular Dysfunction Is Related to Injury to the Inferior Vestibular Nerve. Journal of Neurotrauma, 2022, 39, 829-840.	3.4	6
4	Separating Glioma Hyperintensities From White Matter by Diffusion-Weighted Imaging With Spherical Tensor Encoding. Frontiers in Neuroscience, 2022, 16, 842242.	2.8	0
5	Stay on the Beat With Tensor-Valued Encoding: Time-Dependent Diffusion and Cell Size Estimation in ex vivo Heart. Frontiers in Physics, 2022, 10, .	2.1	3
6	Sensitivity of Diffusion MRI to White Matter Pathology: Influence of Diffusion Protocol, Magnetic Field Strength, and Processing Pipeline in Systemic Lupus Erythematosus. Frontiers in Neurology, 2022, 13, 837385.	2.4	5
7	205: ADJUNCTIVE SURVEILLANCE MODALITIES AND ONCOLOGIC OUTCOME: A REPORT FROM THE ENSURE STUDY. Ecological Management and Restoration, 2022, 35, .	0.4	0
8	Adjuvant radiotherapy for gastric cancer—end of the road?. Annals of Oncology, 2021, 32, 287-289.	1.2	16
9	Gradient waveform design for tensor-valued encoding in diffusion MRI. Journal of Neuroscience Methods, 2021, 348, 109007.	2.5	44
10	Probing tissue microstructure by diffusion skewness tensor imaging. Scientific Reports, 2021, 11, 135.	3.3	6
11	Time dependence in diffusion MRI predicts tissue outcome in ischemic stroke patients. Magnetic Resonance in Medicine, 2021, 86, 754-764.	3.0	14
12	Mortality after surgery for primary hyperparathyroidism: results from a nationwide cohort. British Journal of Surgery, 2021, 108, 858-863.	0.3	5
13	Mapping prostatic microscopic anisotropy using linear and spherical bâ€ŧensor encoding: A preliminary study. Magnetic Resonance in Medicine, 2021, 86, 2025-2033.	3.0	12
14	Magic DIAMOND: Multi-fascicle diffusion compartment imaging with tensor distribution modeling and tensor-valued diffusion encoding. Medical Image Analysis, 2021, 70, 101988.	11.6	9
15	Cortical and white matter correlates of languageâ€learning aptitudes. Human Brain Mapping, 2021, 42, 5037-5050.	3.6	7
16	SPHERIOUSLY? The challenges of estimating sphere radius non-invasively in the human brain from diffusion MRI. NeuroImage, 2021, 237, 118183.	4.2	16
17	On the generalizability of diffusion MRI signal representations across acquisition parameters, sequences and tissue types: Chronicles of the MEMENTO challenge. NeuroImage, 2021, 240, 118367.	4.2	10
18	Neural networks for parameter estimation in microstructural MRI: Application to a diffusion-relaxation model of white matter. NeuroImage, 2021, 244, 118601.	4.2	20

#	Article	IF	CITATIONS
19	Accuracy and precision in super-resolution MRI: Enabling spherical tensor diffusion encoding at ultra-high b-values and high resolution. NeuroImage, 2021, 245, 118673.	4.2	11
20	Tensorâ€valued diffusion MRI in under 3 minutes: an initial survey of microscopic anisotropy and tissue heterogeneity in intracranial tumors. Magnetic Resonance in Medicine, 2020, 83, 608-620.	3.0	55
21	Association between time interval from neoadjuvant chemoradiotherapy to surgery and complete histological tumor response in esophageal and gastroesophageal junction cancer: a national cohort study. Ecological Management and Restoration, 2020, 33, .	0.4	16
22	Tensorâ€valued diffusion MRI differentiates cortex and white matter in malformations of cortical development associated with epilepsy. Epilepsia, 2020, 61, 1701-1713.	5.1	28
23	Blood and cerebrospinal fluid neurofilament light differentially detect neurodegeneration in early Alzheimer's disease. Neurobiology of Aging, 2020, 95, 143-153.	3.1	34
24	Disentangling white-matter damage from physiological fibre orientation dispersion in multiple sclerosis. Brain Communications, 2020, 2, fcaa077.	3.3	55
25	Subjectively Reported Effects Experienced in an Actively Shielded 7T MRI: A Largeâ€Scale Study. Journal of Magnetic Resonance Imaging, 2020, 52, 1265-1276.	3.4	21
26	Towards unconstrained compartment modeling in white matter using diffusionâ€relaxation MRI with tensorâ€valued diffusion encoding. Magnetic Resonance in Medicine, 2020, 84, 1605-1623.	3.0	67
27	Improved fibre dispersion estimation using b-tensor encoding. NeuroImage, 2020, 215, 116832.	4.2	17
28	Motionâ€compensated bâ€ŧensor encoding for in vivo cardiac diffusionâ€weighted imaging. NMR in Biomedicine, 2020, 33, e4213.	2.8	20
29	The dot-compartment revealed? Diffusion MRI with ultra-strong gradients and spherical tensor encoding in the living human brain. NeuroImage, 2020, 210, 116534.	4.2	64
30	Timeâ€dependent diffusion in undulating thin fibers: Impact on axon diameter estimation. NMR in Biomedicine, 2020, 33, e4187.	2.8	31
31	Neoadjuvant chemotherapy versus neoadjuvant chemoradiotherapy for cancer of the esophagus or gastroesophageal junction: long-term results of a randomized clinical trial. Ecological Management and Restoration, 2019, 32, .	0.4	101
32	Multidimensional diffusion MRI with spectrally modulated gradients reveals unprecedented microstructural detail. Scientific Reports, 2019, 9, 9026.	3.3	58
33	Diffusion Tensor MRI to Distinguish Progressive Supranuclear Palsy from α-Synucleinopathies. Radiology, 2019, 293, 646-653.	7.3	20
34	Tensor-valued diffusion encoding for diffusional variance decomposition (DIVIDE): Technical feasibility in clinical MRI systems. PLoS ONE, 2019, 14, e0214238.	2.5	67
35	Maxwellâ€compensated design of asymmetric gradient waveforms for tensorâ€valued diffusion encoding. Magnetic Resonance in Medicine, 2019, 82, 1424-1437.	3.0	81
36	Mapping of apparent susceptibility yields promising diagnostic separation of progressive supranuclear palsy from other causes of parkinsonism. Scientific Reports, 2019, 9, 6079.	3.3	18

#	Article	IF	CITATIONS
37	Monte Carlo Simulations of Water Exchange Through Myelin Wraps: Implications for Diffusion MRI. IEEE Transactions on Medical Imaging, 2019, 38, 1438-1445.	8.9	17
38	Searching for the neurite density with diffusion MRI: Challenges for biophysical modeling. Human Brain Mapping, 2019, 40, 2529-2545.	3.6	103
39	Vancomycin elution from a biphasic ceramic bone substitute. Bone and Joint Research, 2019, 8, 49-54.	3.6	15
40	Shortâ€ŧerm effects experienced during examinations in an actively shielded 7 T MR. Bioelectromagnetics, 2019, 40, 234-249.	1.6	11
41	Microstructural white matter alterations associated to neurocognitive deficits in childhood leukemia survivors treated with cranial radiotherapy – a diffusional kurtosis study. Acta Oncológica, 2019, 58, 1021-1028.	1.8	13
42	O148 SHORT-TERM RESULTS OF A RANDOMIZED CONTROLLED TRIAL OF STANDARD VS. PROLONGED TIME TO SURGERY AFTER NEOADJUVANT CHEMORADIATION FOR CANCER. Ecological Management and Restoration, 2019, 32, .	0.4	0
43	Experiences of specialist social workers for asylum seeking patients at a large Swedish hospital. European Journal of Public Health, 2019, 29, .	0.3	0
44	Characteristics of specialist consultations regarding immigrant patients at a large Swedish hospital. European Journal of Public Health, 2019, 29, .	0.3	0
45	Diagnostic value ofÂalternative techniques to gadolinium-based contrast agents in MR neuroimaging—a comprehensive overview. Insights Into Imaging, 2019, 10, 84.	3.4	44
46	Cortical thickness of Broca's area and right homologue is related to grammar learning aptitude and pitch discrimination proficiency. Brain and Language, 2019, 188, 42-47.	1.6	5
47	Reply to letter: Neoadjuvant chemoradiotherapy or chemotherapy for esophageal cancer: what is the current evidence?. Ecological Management and Restoration, 2019, 32, .	0.4	0
48	Normal radiological lymph node appearance in the thorax. Ecological Management and Restoration, 2019, 32, 1-6.	0.4	4
49	Texture analysis of computed tomography data using morphologic and metabolic delineation of esophageal cancer—relation to tumor type and neoadjuvant therapy response. Ecological Management and Restoration, 2019, 32, .	0.4	11
50	Imaging brain microstructure with diffusion MRI: practicality and applications. NMR in Biomedicine, 2019, 32, e3841.	2.8	266
51	Glioma Grade Discrimination with MR Diffusion Kurtosis Imaging: A Meta-Analysis of Diagnostic Accuracy. Radiology, 2018, 287, 119-127.	7.3	63
52	Alteration of putaminal fractional anisotropy in Parkinson's disease: a longitudinal diffusion kurtosis imaging study. Neuroradiology, 2018, 60, 247-254.	2.2	23
53	Cumulant expansions for measuring water exchange using diffusion MRI. Journal of Chemical Physics, 2018, 148, 074109.	3.0	26
54	Diffusion tensor imaging and tractography of the white matter in normal aging: The rate-of-change differs between segments within tracts. Magnetic Resonance Imaging, 2018, 45, 113-119.	1.8	22

#	Article	IF	CITATIONS
55	Liquid crystal phantom for validation of microscopic diffusion anisotropy measurements on clinical MRI systems. Magnetic Resonance in Medicine, 2018, 79, 1817-1828.	3.0	18
56	Assessing Tissue Heterogeneity by non-Gaussian Measures in a Permeable Environment. , 2018, , .		1
57	Brain Tumor Characterization Using Multibiometric Evaluation of MRI. Tomography, 2018, 4, 14-25.	1.8	12
58	The KÃ ¤ ger vs bi-exponential model: Theoretical insights and experimental validations. Journal of Magnetic Resonance, 2018, 296, 72-78.	2.1	18
59	Effects of APOE ε4 on neuroimaging, cerebrospinal fluid biomarkers, and cognition in prodromal Alzheimer's disease. Neurobiology of Aging, 2018, 71, 81-90.	3.1	15
60	Imaging brain tumour microstructure. NeuroImage, 2018, 182, 232-250.	4.2	62
61	Altered white matter microstructure in lupus patients: a diffusion tensor imaging study. Arthritis Research and Therapy, 2018, 20, 21.	3.5	28
62	Single center consecutive series cohort study of minimally invasive versus open resection for cancer in the esophagus or gastroesophageal junction. Ecological Management and Restoration, 2018, 31, .	0.4	13
63	Regional structural hypo―and hyperconnectivity of frontal–striatal and frontal–thalamic pathways in behavioral variant frontotemporal dementia. Human Brain Mapping, 2018, 39, 4083-4093.	3.6	21
64	Neurite density imaging versus imaging of microscopic anisotropy in diffusion MRI: A model comparison using spherical tensor encoding. NeuroImage, 2017, 147, 517-531.	4.2	177
65	Diffusion MRI microstructure models with in vivo human brain Connectome data: results from a multiâ€group comparison. NMR in Biomedicine, 2017, 30, e3734.	2.8	33
66	Resolution limit of cylinder diameter estimation by diffusion MRI: The impact of gradient waveform and orientation dispersion. NMR in Biomedicine, 2017, 30, e3711.	2.8	116
67	Optimal experimental design for filter exchange imaging: Apparent exchange rate measurements in the healthy brain and in intracranial tumors. Magnetic Resonance in Medicine, 2017, 77, C1-C1.	3.0	2
68	Optimal experimental design for filter exchange imaging: Apparent exchange rate measurements in the healthy brain and in intracranial tumors. Magnetic Resonance in Medicine, 2017, 77, 1104-1114.	3.0	67
69	The effect of white matter hyperintensities on statistical analysis of diffusion tensor imaging in cognitively healthy elderly and prodromal Alzheimer's disease. PLoS ONE, 2017, 12, e0185239.	2.5	32
70	Diffusion kurtosis imaging of gliomas grades II and III - a study of perilesional tumor infiltration, tumor grades and subtypes at clinical presentation. Radiology and Oncology, 2017, 51, 121-129.	1.7	37
71	Umfangreiche epidemiologische und Genotyp-Phäotyp (GxP) Analysen in dem weltweit größten Patientenkollektiv mit idiopathischer Achalasie. Zeitschrift Fur Gastroenterologie, 2017, 55, .	0.5	0
72	Preoperative Quantitative MR Tractography Compared with Visual Tract Evaluation in Patients with Neuropathologically Confirmed Gliomas Grades II and III: A Prospective Cohort Study. Radiology Research and Practice, 2016, 2016, 1-15.	1.3	6

#	Article	IF	CITATIONS
73	Grey and White Matter Clinico-Anatomical Correlates of Disinhibition in Neurodegenerative Disease. PLoS ONE, 2016, 11, e0164122.	2.5	15
74	Pharmacokinetics of gentamicin eluted from a regenerating bone graft substitute. Bone and Joint Research, 2016, 5, 427-435.	3.6	67
75	Scintillate: An open-source graphical viewer for time-series calcium imaging evaluation and pre-processing. Journal of Neuroscience Methods, 2016, 273, 120-127.	2.5	1
76	The link between diffusion MRI and tumor heterogeneity: Mapping cell eccentricity and density by diffusional variance decomposition (DIVIDE). NeuroImage, 2016, 142, 522-532.	4.2	141
77	Outcome of neoadjuvant therapies for cancer of the oesophagus or gastro-oesophageal junction based on a national data registry. British Journal of Surgery, 2016, 103, 1864-1873.	0.3	26
78	Conventions and nomenclature for double diffusion encoding NMR and MRI. Magnetic Resonance in Medicine, 2016, 75, 82-87.	3.0	154
79	Apparent exchange rate for breast cancer characterization. NMR in Biomedicine, 2016, 29, 631-639.	2.8	36
80	Quantification of microcirculatory parameters by joint analysis of flowâ€compensated and nonâ€flowâ€compensated intravoxel incoherent motion (IVIM) data. NMR in Biomedicine, 2016, 29, 640-649.	2.8	72
81	Systematic review and meta-analysis on the significance of salvage esophagectomy for persistent or recurrent esophageal squamous cell carcinoma after definitive chemoradiotherapy. Ecological Management and Restoration, 2016, 29, 734-739.	0.4	42
82	A randomized clinical trial of neoadjuvant chemotherapy versus neoadjuvant chemoradiotherapy for cancer of the oesophagus or gastro-oesophageal junction. Annals of Oncology, 2016, 27, 660-667.	1.2	300
83	Q-space trajectory imaging for multidimensional diffusion MRI of the human brain. NeuroImage, 2016, 135, 345-362.	4.2	256
84	Alterations of Diffusion Kurtosis and Neurite Density Measures in Deep Grey Matter and White Matter in Parkinson's Disease. PLoS ONE, 2016, 11, e0157755.	2.5	35
85	NMR diffusion-encoding with axial symmetry and variable anisotropy: Distinguishing between prolate and oblate microscopic diffusion tensors with unknown orientation distribution. Journal of Chemical Physics, 2015, 142, 104201.	3.0	70
86	Evaluation of small-volume tubes for venous and capillary PT (INR) samples. International Journal of Laboratory Hematology, 2015, 37, 699-704.	1.3	4
87	Comparison of Macular Thickness in Patients with Keratoconus and Control Subjects Using the Cirrus HD-OCT. BioMed Research International, 2015, 2015, 1-5.	1.9	8
88	Morbidity and mortality after surgery for cancer of the oesophagus and gastro-oesophageal junction: A randomized clinical trial of neoadjuvant chemotherapy vs. neoadjuvant chemoradiation. European Journal of Surgical Oncology, 2015, 41, 920-926.	1.0	86
89	Constrained optimization of gradient waveforms for generalized diffusion encoding. Journal of Magnetic Resonance, 2015, 261, 157-168.	2.1	106
90	Survival benefit and additional value of preoperative chemoradiotherapy in resectable gastric and gastro-oesophageal junction cancer: A direct and adjusted indirect comparison meta-analysis. European Journal of Surgical Oncology, 2015, 41, 282-294.	1.0	33

#	Article	IF	CITATIONS
91	Evaluation of the anterior chamber angle in keratoconus and normal subjects. Contact Lens and Anterior Eye, 2015, 38, 277-282.	1.7	3
92	Disease-specific structural changes in thalamus and dentatorubrothalamic tract in progressive supranuclear palsy. Neuroradiology, 2015, 57, 1079-1091.	2.2	37
93	Quantification of microscopic diffusion anisotropy disentangles effects of orientation dispersion from microstructure: Applications in healthy volunteers and in brain tumors. NeuroImage, 2015, 104, 241-252.	4.2	216
94	Extrapolation-Based References Improve Motion and Eddy-Current Correction of High B-Value DWI Data: Application in Parkinson's Disease Dementia. PLoS ONE, 2015, 10, e0141825.	2.5	75
95	Objective assessment of cataract: Comparison between the Lens Opacities Classification System III and a Scheimpflug camera. Acta Ophthalmologica, 2015, 93, n/a-n/a.	1.1	0
96	Use of directional optical coherence tomography and selected landmarks to determine foveal topography and microstructure. A strategy to characterize differences between normal and expremature cases. Acta Ophthalmologica, 2015, 93, n/a-n/a.	1.1	0
97	Reduced retinal nerve fibre layer thickness in multiple sclerosis patients with and without history of optic neuritis. Acta Ophthalmologica, 2015, 93, n/a-n/a.	1.1	0
98	Microanisotropy imaging: quantification of microscopic diffusion anisotropy and orientational order parameter by diffusion MRI with magic-angle spinning of the q-vector. Frontiers in Physics, 2014, 2, .	2.1	163
99	Reproducibility of psychophysics and electroencephalography during offset analgesia. European Journal of Pain, 2014, 18, 824-834.	2.8	15
100	Intravoxel incoherent motion (IVIM) imaging at different magnetic field strengths: What is feasible?. Magnetic Resonance Imaging, 2014, 32, 1247-1258.	1.8	23
101	Measurement Tensors in Diffusion MRI: Generalizing the Concept of Diffusion Encoding. Lecture Notes in Computer Science, 2014, 17, 209-216.	1.3	55
102	Improved analysis of the outer foveal microstructure - OCT imaging of healthy and abnormal retina. Acta Ophthalmologica, 2014, 92, 0-0.	1.1	0
103	Noninvasive mapping of water diffusional exchange in the human brain using filterâ€exchange imaging. Magnetic Resonance in Medicine, 2013, 69, 1572-1580.	3.0	142
104	Variability in diffusion kurtosis imaging: Impact on study design, statistical power and interpretation. NeuroImage, 2013, 76, 145-154.	4.2	62
105	Spatial analysis of diffusion tensor tractography statistics along the inferior fronto-occipital fasciculus with application in progressive supranuclear palsy. Magnetic Resonance Materials in Physics, Biology, and Medicine, 2013, 26, 527-537.	2.0	18
106	The role of tissue microstructure and water exchange in biophysical modelling of diffusion in white matter. Magnetic Resonance Materials in Physics, Biology, and Medicine, 2013, 26, 345-370.	2.0	123
107	Regional values of diffusional kurtosis estimates in the healthy brain. Journal of Magnetic Resonance Imaging, 2013, 37, 610-618.	3.4	71
108	Assessment of Global and Regional Diffusion Changes along White Matter Tracts in Parkinsonian Disorders by MR Tractography. PLoS ONE, 2013, 8, e66022.	2.5	29

#	Article	IF	CITATIONS
109	Diffusion Tensor Tractography versus Volumetric Imaging in the Diagnosis of Behavioral Variant Frontotemporal Dementia. PLoS ONE, 2013, 8, e66932.	2.5	44
110	The importance of axonal undulation in diffusion MR measurements: a Monte Carlo simulation study. NMR in Biomedicine, 2012, 25, 795-805.	2.8	142
111	Can restingâ€state functional MRI serve as a complement to taskâ€based mapping of sensorimotor function? A test–retest reliability study in healthy volunteers. Journal of Magnetic Resonance Imaging, 2011, 34, 511-517.	3.4	34
112	Apparent exchange rate mapping with diffusion MRI. Magnetic Resonance in Medicine, 2011, 66, 356-365.	3.0	102
113	Clinical importance of spherical and chromatic aberration on the accommodative response in contact lens wear. Journal of Modern Optics, 2011, 58, 1696-1702.	1.3	5
114	Evaluating the accuracy and precision of a two-compartment KÃ r ger model using Monte Carlo simulations. Journal of Magnetic Resonance, 2010, 206, 59-67.	2.1	51
115	Assessment of spatial BOLD sensitivity variations in fMRI using gradient-echo field maps. Magnetic Resonance Imaging, 2010, 28, 947-956.	1.8	3
116	Dimensionality reduction of fMRI time series data using locally linear embedding. Magnetic Resonance Materials in Physics, Biology, and Medicine, 2010, 23, 327-338.	2.0	19
117	Multicomponent Interdiffusion and Self-Diffusion of the Cationic Poly{[9,9-bis(6′- <i>N</i> , <i>N</i> , <i>N</i> -trimethylammonium)hexyl]fluorene-phenylene} Dibromide in a Dimethyl Sulfoxide + Water Solution. Journal of Chemical & Engineering Data, 2010, 55, 1860-1866.	1.9	18
118	Diffusionâ€weighted MRI measurements on stroke patients reveal waterâ€exchange mechanisms in subâ€acute ischaemic lesions. NMR in Biomedicine, 2009, 22, 619-628.	2.8	38
119	Filter-exchange PGSE NMR determination of cell membrane permeability. Journal of Magnetic Resonance, 2009, 200, 291-295.	2.1	93
120	On the effects of a varied diffusion time in vivo: is the diffusion in white matter restricted?. Magnetic Resonance Imaging, 2009, 27, 176-187.	1.8	88
121	In vivo visualization of displacement-distribution-derived parameters in q-space imaging. Magnetic Resonance Imaging, 2008, 26, 77-87.	1.8	43
122	Vertical imbalance induced by prism-ballasted soft toric contact lenses fitted unilaterally. Ophthalmic and Physiological Optics, 2008, 28, 157-162.	2.0	7
123	Thermodynamic and Kinetic Characterization of Hostâ^'Guest Association between Bolaform Surfactants and α- and β-Cyclodextrins. Journal of Physical Chemistry B, 2008, 112, 11310-11316.	2.6	63
124	Molecular Exchange between Intra- and Extracellular Compartments in a Cell Suspension. , 2008, , .		1
125	Accuracy of \$q\$-Space Related Parameters in MRI: Simulations and Phantom Measurements. IEEE Transactions on Medical Imaging, 2007, 26, 1437-1447.	8.9	39
126	Early detection of macular changes in patients with diabetes using Rarebit Fovea Test and optical coherence tomography. British Journal of Ophthalmology, 2007, 91, 1596-1598.	3.9	59

#	Article	IF	CITATIONS
127	Effects of restricted diffusion in a biological phantom: a q-space diffusion MRI study of asparagus stems at a 3T clinical scanner. Magnetic Resonance Materials in Physics, Biology, and Medicine, 2007, 20, 213-222.	2.0	34
128	Interactions between Gemini Surfactants, 12-s-12, and β-cyclodextrin As Investigated by NMR Diffusometry and Electric Conductometry. Langmuir, 2006, 22, 8663-8669.	3.5	53
129	Perception of very small visual stimuli in the fovea: normative data for the Rarebit Foveal Test. Australasian journal of optometry, The, 2006, 89, 81-85.	1.3	14
130	Lifestyle related risk factors in the aetiology of gastro-oesophageal reflux. Gut, 2004, 53, 1730-1735.	12.1	258
131	Prevalence of gastro-oesophageal reflux symptoms and the influence of age and sex. Scandinavian Journal of Gastroenterology, 2004, 39, 1040-1045.	1.5	100
132	Biodegradation and biocompatability of a calcium sulphate-hydroxyapatite bone substitute. Journal of Bone and Joint Surgery: British Volume, 2004, 86-B, 120-125.	3.4	95
133	Biodegradation and biocompatability of a calcium sulphate-hydroxyapatite bone substitute. Journal of Bone and Joint Surgery: British Volume, 2004, 86, 120-5.	3.4	31
134	Body Mass and Reflux Oesophagitis: an Oestrogen-dependent Association?. Scandinavian Journal of Gastroenterology, 2002, 37, 626-630.	1.5	134
135	Feeling old: being in a phase of transition in later life. Nursing Inquiry, 2000, 7, 41-49.	2.1	59
136	Induction of basal cell carcinomas and trichoepitheliomas in mice overexpressing GLI-1. Proceedings of the United States of America, 2000, 97, 3438-3443.	7.1	352
137	Solid phase ELISA for serum ferritin. Scandinavian Journal of Clinical and Laboratory Investigation, 1980, 40, 641-645.	1.2	1
138	Macular abnormalities and the Rarebit Fovea Test. Acta Ophthalmologica, 0, 85, 0-0.	0.3	0
139	Foveal function in children treated for amblyopia. Acta Ophthalmologica, 0, 85, 0-0.	0.3	1